Pergamon

Chemical Engineering Science, Vol. 53, No. 4, pp. 787–805, 1998

Printed in Great Britain
0009-2509/98 $19.00 + 0.00

PII: S0009-2509(97)00366-7

A trickle-bed reactor model for hydrogenation of 2,4 dinitrotoluene: experimental verification

Malyala V. Rajashekharam, Rengaswamy Jaganathan and Raghunath V. Chaudhari*

Chemical Engineering Division, National Chemical Laboratory, Pune 411 008, India

(Received 12 November 1996)

Abstract—A trickle-bed reactor model has been developed for hydrogenation of 2,4 dinitrotoluene (DNT). This model incorporates the contributions of partial wetting and stagnant liquid hold-up effects in addition to external and intraparticle mass transfer resistances for a complex consecutive/parallel reaction scheme under consideration represented by L-H-type kinetics. As the reaction is highly exothermic, the heat effects have also been incorporated in the model. The reactor performance for complete wetting, partial wetting of catalyst particles and in the presence of stagnant liquid pockets has been compared and the significance of different parameters discussed. Experimental data were obtained for different particles sizes, different gas and liquid velocities in a temperature range 318–328 K. The model predictions were compared with experimental data and were found to agree very well for a wide range of operating conditions. The model proposed here also allowed prediction of maximum temperature rise in the catalyst bed and which was also found to agree well with the steady-state experimental data. Under certain conditions, hysteresis behaviour of the reactor performance has been observed.

Keywords: Trickle bed reactor; hydrogenation.

INTRODUCTION

Trickle-bed reactors wherein gas and liquid reactants are contacted in a co-current down flow mode in the presence of heterogeneous catalysts are used in a large number of industrial chemical processes. Being a multiphase catalytic reactor with complex hydrodynamics and mass transfer characteristics, the development of a generalized model for such reactors is still a difficult task. However, due to its direct relevance to industrial-scale processes, several important aspects with respect to the influence of external and intraparticle mass transfer effects, partial wetting of catalyst particles and heat effects have been studied previously (Satterfield and Way, 1972; Hanika *et. al.*, 1975, 1977, 1981; Herskowitz and Mosseri, 1983). The previous work has mainly addressed the question of catalyst effectiveness under isothermal conditions and for simple first-order kinetics. It is well known that most of the industrially important reactions represent complex reaction kinetics and very often multistep reactions. In addition, these reactions are highly exothermic and control of temperature is a major design problem. Very few attempts have been made on experimental verification of trickle-bed reactor models for exothermic multistep catalytic reactions in the previous work.

The analysis of mass transfer effects in a trickle-bed reactor has been extensively studied and the relevant literature on this subject has been reviewed by Satterfield (1975), Herskowitz and Smith (1983), Ramachandran and Chaudhari (1983), Mills and Dudukovic (1984), and Gianetto and Specchia (1992). Several models have been proposed to describe the influence of partial external wetting of catalyst particles (Ramachandran and Smith, 1979; Herskowitz *et al.*, 1979; Tan and Smith, 1980; Mills and Dudukovic, 1980; Goto *et al.*, 1981). These models predict that the overall rate of reaction increases under conditions of partial wetting for a gas limited reaction, due to the elimination of liquid-particle mass transfer step for the unwetted part of the catalyst particles. Unlike partial wetting, the role of stagnant liquid pockets in between the catalyst particles has not received much attention. It is well known that in trickle-bed reactors, a significant fraction of the liquid hold-up can remain as stagnant pools [as much as 20–30% of the total area of the catalyst particle can be covered by stagnant zones (Sicardi *et al.*, 1980; Colombo *et al.*, 1976; Koros, 1986). Heat effects and the hysteresis phenomenon due to vaporization of liquid phase in trickle

*Corresponding author. Tel.: 00 91 212 346135; fax: 00 91 212 333941; e-mail: rvc@ncl.ernet.in.

Table 1. A summary of literature on the experimental verification of trickle-bed reactor models

No.	Reaction system	Rate analysis	Features considered in the model	Reference
1	SO_2 oxidation	Linear kinetics	Plug flow, isothermal, partial wetting (wetting efficiency is an adjustable parameter)	Hartmann and Coughlin (1972)
2	Hydrodesulphurization of Kuwait crude oil	First order kinetics	Pseudo-homogeneous model, isothermal,	Paraskos *et al.* (1975), Shah and Paraskos (1975), Montagna and Shah (1975)
3	Formic acid oxidation	Linear kinetics	Axial dispersion, isothermal, partial wetting	Goto and Smith (1975)
4	Acetic acid oxidation	L-H-type kinetics	Axial dispersion, isothermal, partial wetting	Levec and Smith (1976)
5	Hydrodesulphurization of petroleum oil	First-order kinetics	Plug flow, isothermal, heat balance accounted for	Shah *et al.* (1976)
6	SO_2 oxidation	Linear kinetics	Axial dispersion, isothermal, partial wetting	Mata and Smith (1981)
7	α-methyl styrene hydrogenation	Linear kinetics	Plug flow, isothermal, partial wetting	Mills and Dudukovic (1984)
8	Xylose hydrogenation	Linear kinetics	Plug flow, isothermal, partial wetting	Herskowitz (1985)
9	α-methyl styrene and maleic acid hydrogenation	Linear kinetics	Plug flow, isothermal, partial wetting, liquid diffusional limitations	Beaudry *et al.* (1987)
10	Benzaldehyde hydrogenation	L-H-type kinetics	Plug flow, isothermal, partial wetting	Herskowitz (1988)
11	Isobutene hydration	Linear kinetics	Isothermal, complete wetting, heat balance and pressure drop accounted for	Caceres *et al.* (1988)
12	Decomposition of H_2O_2	Linear kinetics	Isothermal, two region cell reactor model, partial wetting	Brad Sims *et al.* (1994)
13	Hydrogenation of 3-hydroxy propanal	L-H-type kinetics	Plug flow, isothermal, partial wetting, heat balance accounted for	Valerius *et al.* (1996)
14	Hydrotreating of vacuum gas oil	L-H-type kinetics	Isothermal, plug flow, partial wetting	Korsten and Hoffmann (1996)

beds for exothermic reactions such as hydrogenation of α-methyl styrene, cyclooctadiene and cyclohexene have been reported by Germain *et al.* (1974) and Hanika *et al.* (1981). For a single-pellet reactor, experimental data on hydrogenation of α-methyl styrene and cyclohexene have been compared with model predictions under both isothermal as well as non-isothermal conditions (Funk *et al.*, 1991; Harold and Ng, 1993; Watson and Harold, 1993, 1994). It was also concluded that the wetting efficiency (defined as the fraction of the catalyst wetted by the flowing liquid) can change due to the vaporization of the solvent (for an exothermic reaction) causing external dewetting of the catalyst particles.

From a practical point of view it is important to incorporate the complexities of hydrodynamics and mass transfer steps coupled with a catalytic reaction in a model for the entire reactor under integral conditions. Several reports on modelling of trickle-bed reactors have been published with the aim of understanding the overall reactor performance and comparison of the predictions with experimental data (Goto and Smith, 1975; Levec and Smith, 1976; Herskowitz, 1985 among others). A summary of literature on experimental verification of trickle-bed reactor models is shown in Table 1. These studies reveal that in most cases single reactions with simplified rate equations were considered under isothermal conditions. There is practically no published report on modelling of a trickle-bed reactor for a complex multistep reaction system under non-isothermal conditions.

This paper reports an experimental verification of a non-isothermal trickle-bed reactor model for hydrogenation of 2, 4 dinitrotoluene (DNT) which represents a case of highly exothermic [$-\Delta H = 556$ kJ/mol of nitro group (McNab, 1981)] catalytic reaction involving parallel and consecutive steps, and is industrially important reaction for the manufacture of toluene diisocyanate (TDI) and polyurethanes. Since there are many examples of industrial relevance wherein multistep exothermic reactions are carried out in a trickle-bed reactor, it was thought important to undertake a detailed study on experimental verification of a trickle-bed reactor model for hydrogenation of DNT. The kinetics of hydrogenation of DNT using supported Pd catalysts has been studied earlier by Janssen *et al.* (1990a,b), Molga and Westerterp (1992), Nikalje (1993) and Neri *et al.* (1995). In most cases it has been observed that the reaction follows a L-H-type mechanism and the reaction rate is first order tending to zero order with respect to H_2 pressure and zero order with respect to DNT. The hydrogenation of DNT in a continuously stirred-tank reactors (CSTR) has been studied by Westerterp *et al.* (1992) and a mathematical model has been proposed by Janssen *et al.* (1992) to predict the performance of a CSTR for hydrogenation of DNT incorporating the effect of an evaporating solvent. To the best of our knowledge this reaction system has not been investigated in a trickle-bed reactor under integral conditions and the modelling of a non-isothermal trickle-bed reactor applicable to hydrogenation of DNT has not been reported so far. The model developed in this work is based on the extended approach of Tan and Smith (1980), for a complex multistep reaction to predict the overall performance of a trickle-bed reactor incorporating partial wetting and stagnant liquid hold-up effects. The temperature dependence of different parameters such as saturation solubility, effective diffusivity, reaction rate and equilibrium constants is incorporated in the model. For the purpose of experimental verification of a trickle-bed reactor model, the hydrogenation of DNT was carried out using a 5% Pd/Al_2O_3 catalyst pellets. Experimental data on the effect of liquid velocity on the global rates of hydrogenation, DNT conversion, TDA selectivity and maximum temperature rise was obtained for different particle sizes in a temperature range 318–328 K. Also, the effect of gas velocity on the global rate of hydrogenation was studied. The experimental data have been compared with the model predictions for different sets of conditions and relative importance of different parameters discussed.

EXPERIMENTAL

The experiments were carried out in a trickle-bed reactor supplied by 'Geomechanique', France. The schematic of the reactor set-up is shown in Fig. 1. The reactor consists of a stainless-steel tube of 0.3 m length and 1.5×10^{-2} m inner diameter. The reactor was provided with two thermocouples [Chromel-Alumel thermocouples (type K)] to measure temperatures at two different points, one at the entrance of the reactor and the other at the centre of the catalyst bed. The reactor was equipped with mass flow controllers, and pressure indicator and controller (PIC) devices. A storage tank was connected to the metering pump through a volumetric burette in order to measure the liquid feed rate. The pump had a maximum capacity of 3×10^{-4} m^3/h, under a pressure of 10 MPa. The other end of the reactor was connected to a gas–liquid separator through a condenser.

DNT obtained from M/s Fluka, Switzerland was thoroughly dried to remove moisture before use. 2-Amino-4-nitrotoluene (2A4NT) and 4-amino-2-nitrotoluene (4A2NT) from M/s Fluka, Switzerland and TDA from M/s Aldrich, U.S.A., were used in quantitative gas chromatography analysis as authentic samples. The solvent ethyl acetate was obtained from M/s S. D. Fine Chemicals, India and was freshly distilled before use. H_2 and N_2 gases were obtained from M/s Indian Oxygen Ltd, India, were directly used without further purification. The catalyst was prepared by the procedure described by Mozingo (1956). The precursor of the catalyst $PdCl_2$ was supplied by Arora Matthey, India, and the support activated alumina (Puralox SCFA-240) from M/s Condea Chemie, Germany. The powdered catalyst was pelletized and sieved through standard test sieves to obtain desired particle sizes (1×10^{-3} and 2×10^{-3} m).

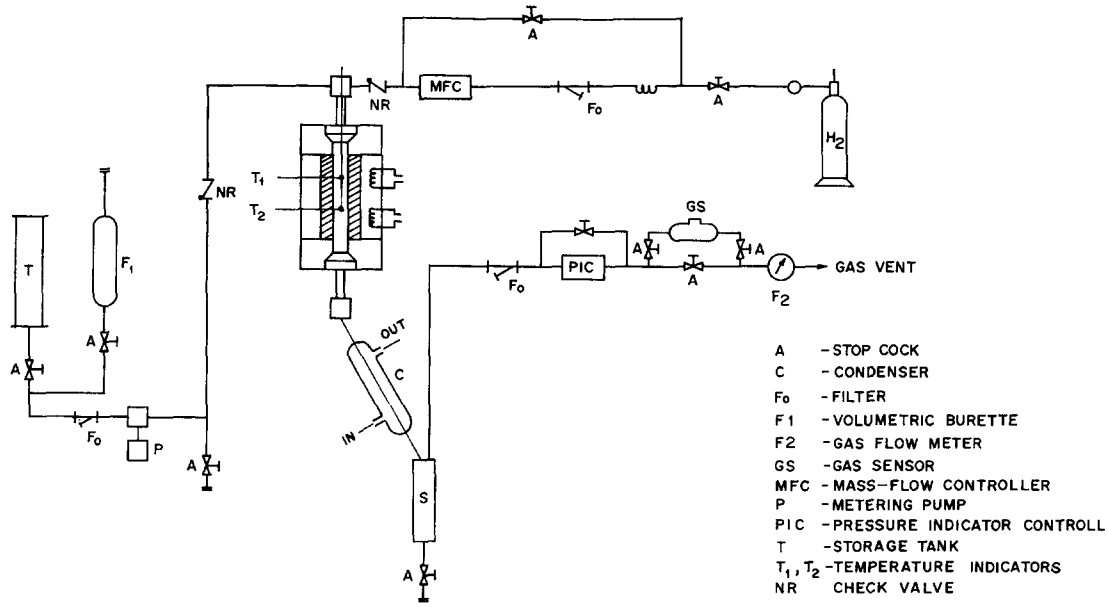

Fig. 1. A schematic of the trickle-bed reactor set-up.

Table 2. Operating conditions of the trickle-bed reactor

Catalyst	5% Pd/Al_2O_3
Weight of the catalyst, W	9×10^{-3} kg
Initial concentration of DNT, B_{li}	0.2–0.5 kmol/m^3
H_2 pressure	1.4 and 3 MPa
Solvent	Ethyl acetate
Liquid velocity, U_l	$1–50 \times 10^{-5}$ m/s
Gas velocity, U_g	$2–6 \times 10^{-3}$ m/s
Reactor diameter, d_T	1.5×10^{-2} m
Total reactor length	0.3 m
Catalyst packing length, L	5.67×10^{-2} m
Bed voidage, ε_B	0.5
Particle diameter, d_p	1×10^{-3} and 2×10^{-3} m
Density of the catalyst, ρ_p	1.8×10^3 kg/m^3
Porosity of the catalyst, ε	0.3
Tourtosity of the catalyst, τ	7.5

In each experiment, 9×10^{-3} kg of catalyst was charged in the reactor, wherein the sections above and below the catalyst bed were packed with inert packing (carborundum). The reactor was flushed thoroughly with N_2 and then with H_2 at room temperature before start of actual experiment. After attaining the desired temperature the reactor was pressurized with H_2. The liquid feed was 'switched on' after the reactor has reached the operating pressure. Liquid samples were withdrawn at regular intervals of time and were analysed by gas chromatography (Varian, 3600) using a 5% Dexil 300 on chromosorb W column of 1 m length. The liquid velocity was changed after confirming the steady-state achievement from the GC analysis. Following this procedure, experiments were carried out at different inlet conditions and steady-state performance of the reactor observed by analysis of reactants and products in the exit streams. The range of operating conditions studied are listed in Table 2.

MATHEMATICAL MODEL

For the purpose of developing a trickle-bed reactor model for hydrogenation of DNT, the rate equations proposed earlier by Nikalje (1993) were used. He studied the intrinsic kinetics of the reaction in detail and showed the validity of the rate equations proposed under integral conditions. The following rate equations were proposed by him based on the rate data in a slurry reactor to represent the intrinsic kinetics of different reaction steps shown in Fig. 2:

$$r_1 = \frac{W k_1 A^* B_l}{(1 + K_A A^* + K_B B_l + K_C C_l + K_E E_l)} \quad (1)$$

$$r_2 = \frac{W k_2 A^* B_l}{(1 + K_A A^* + K_B B_l + K_C C_l + K_E E_l)} \quad (2)$$

$$r_3 = \frac{W k_3 A^* C_l}{(1 + K_A A^* + K_B B_l + K_C C_l + K_E E_l)} \quad (3)$$

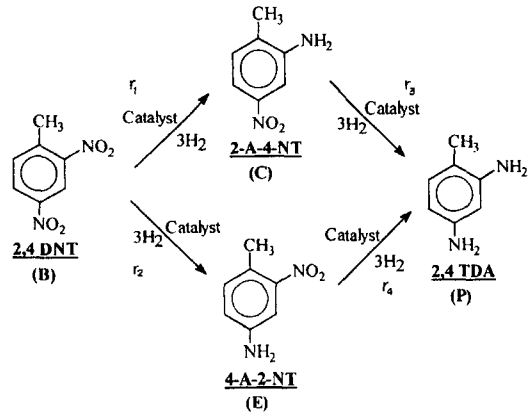

Fig. 2. Reaction scheme for hydrogenation of 2,4 DNT.

$$r_4 = \frac{W k_1 A^* E_l}{(1 + K_A A^* + K_B B_l + K_C C_l + K_E E_l)}. \quad (4)$$

The overall rate of hydrogenation can be given as

$$R_A = \frac{W(k_1 B_l + k_2 B_l + k_3 C_l + k_4 E_l) A^*}{(1 + K_A A^* + K_B B_l + K_C C_l + K_E E_l)} \quad (5)$$

where A represents H_2 and B_l, C_l and E_l represent the concentration of DNT, 2A4NT and 4A2NT. The different kinetic parameters and activation energy values evaluated for the above rate equations are given in Tables 3 and 4. The catalyst used for experimental study in a trickle-bed reactor in this work was the same as used by Nikalje (1993) except that the powder catalyst was pelletized for trickle-bed reactor experiments. Therefore, the rate equations given above were considered as most appropriate for the present work.

Assumptions of the model

For the purpose of developing a trickle-bed reactor model applicable to hydrogenation of DNT, the approach of Tan and Smith (1980) was used to evaluate an approximate solution of the catalytic effectiveness factor under conditions of partial wetting and in the presence of significant stagnant liquid pockets in between the catalyst particles. The spherical catalyst particle was assumed to be divided into three zones as shown in Fig. 3: (1) a dry zone, (2) a wetted zone covered by the flowing dynamic liquid and (3) a wetted zone covered by the stagnant liquid. It is assumed that (a) gas and liquid are in plug flow; (b) liquid-phase reactant is non-volatile and is in excess when compared to the gaseous reactant; (c) the gas–liquid, liquid–solid and intraparticle mass transfer resistances for H_2 are considered, whereas the liquid–solid and intraparticle mass transfer resistances for the liquid-phase components are assumed to be negligible; (d) the interphase and intraparticle heat transfer resistances are negligible; (e) the overall catalytic effectiveness factor can be expressed as a sum of the weighted average of the effectiveness factor in the dynamic covered, stagnant liquid covered and complete gas covered zones, respectively, i.e.,

$$\eta_c = f_d \eta_{c_d} + f_s \eta_{c_s} + (1 - f_d - f_s)\eta_{c_g} \quad (6)$$

where η_c is the overall catalytic effectiveness factor, f_d and f_s are the fractions of the catalyst particle covered by the dynamic and stagnant zones and η_{c_d}, η_{c_s} and η_{c_g} are the catalytic effectiveness factors in the dynamic, stagnant and dry zones, respectively, (f) the overall rate of hydrogenation is first-order with respect to hydrogen. For the reaction conditions used in this work, the term $K_A A^*$ is very much less than 1 and hence, first order with H_2 can be assumed for simplicity; and (h) the catalyst is wetted completely internally due to capillary forces.

The catalytic effectiveness factor equations applicable to hydrogenation of DNT can be developed following the well-known approaches (Ramachandran and Chaudhari, 1983; and Bischoff, 1965). Under the conditions of significant intraparticle gradients for the gas-phase reactant (H_2) and when the liquid-phase reactant is in excess, the following equations can be used.

The overall rate of hydrogenation can now be expressed as

$$R_A = \frac{\eta_c W(k_1 B_l + k_2 B_l + k_3 C_l + k_4 E_l) A^*}{(1 + K_B B_l + K_C C_l + K_E E_l)} \quad (7)$$

where η_c is the overall catalytic effectiveness factor and for a spherical catalyst particle expressed as

$$\eta_c = \frac{1}{\phi}\left(\coth 3\phi - \frac{1}{3\phi}\right). \quad (8)$$

Here ϕ is the Thiele parameter and is given by

$$\phi = \frac{R}{3}\left[\frac{S_p(k_1 B_l + k_2 B_l + k_3 C_l + k_4 E_l)}{D_e(1 + K_B B_l + K_C C_l + K_E E_l)}\right]^{1/2} \quad (9)$$

Table 3. Kinetic parameters for hydrogenation of DNT

	Rate constants × 10^2(m^3/kg) (m^3/kmol) s^{-1}				Adsorption constants × 10^3(m^3/kmol)			
Temperature (K)	k_1	k_2	k_3	k_4	K_A	K_B	K_C	K_D
313	1.62	1.26	0.05	2.39	0.29	5.56	0.95	2.84
323	3.32	2.36	0.93	3.93	0.52	8.01	1.31	4.53
343	10.77	6.79	2.45	9.11	0.94	15.06	1.81	4.23
363	34.40	16.87	8.19	17.96	2.71	23.26	3.27	6.80

Table 4. Activation parameters

Activation energy, E_1	65.68 kJ/mol
Activation energy, E_2	53.00 kJ/mol
Activation energy, E_3	56.77 kJ/mol
Activation energy, E_4	41.65 kJ/mol
Heat of adsorption of hydrogen ($-\Delta H_A$)	49.44 kJ/mol
Heat of adsorption of DNT ($-\Delta H_B$)	30.72 kJ/mol
Heat of adsorption of 2A-4-NT ($-\Delta H_C$)	27.11 kJ/mol
Heat of adsorption of 4A-2-NT ($-\Delta H_E$)	39.26 kJ/mol

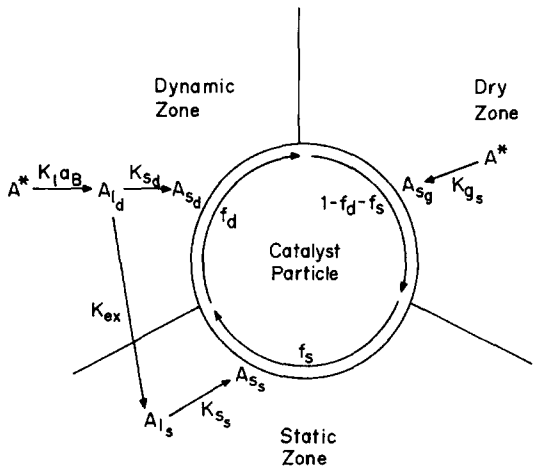

Fig. 3. Spherical catalyst particle shown as divided in three zones.

or, in terms of dimensionless concentrations,

$$\phi = \phi_o \left[\frac{(b_l + k_{21} b_l + k_{31} c_l + k_{41} e_l)}{(1 + k_b b_l + k_c c_l + k_e e_l)} \right]^{1/2} \quad (10)$$

with

$$\phi_o = \frac{R}{3} \left[\frac{\rho_p k_1 B_{l_i}}{D_e} \right]^{1/2}. \quad (11)$$

The dimensionless parameters used in expressing ϕ are listed in Table 5. The mass balance of H_2 in the dynamic liquid phase is given as

$$-U_l \frac{dA_{l_d}}{dx} + k_l a_B (A^* - A_{l_d}) = K_{ex} \varepsilon_{l_s} (A_{l_d} - A_{l_s}) + f_d k_{s_d} a_p (A_{l_d} - A_{s_d}). \quad (12)$$

At steady-state conditions, the sum of the convection term and the gas–liquid mass transfer term are in equilibrium with the liquid–solid mass transfer term in the dynamic zone and the volumetric mass exchanged between the dynamic and stagnant zones. In a previous study by Hochmann and Effron (1969), it was shown that the exchange rates between the dynamic and stagnant zones can be explained by a volumetric mass exchange coefficient, K_{ex}, and with the help of a cross flow model. Thus, in the dynamic zone

Table 5. Dimensionless parameters used in the model

Mass transfer parameters	
Gas–liquid mass transfer	$\alpha_{gl} = k_l a_B L/U_l$
Liquid–solid mass transfer	$\alpha_{ls} = k_s a_p L/U_l$
Gas–solid mass transfer	$\alpha_{gs} = k_{g_s} a_p L/U_l$
Nusslet number in dynamic zone	$N_d = Rk_{s_d}/3D_e$
Nusslet number in stagnant zone	$N_s = Rk_{s_s}/3D_e$
Nusslet number in dry zone	$N_g = Rk_{g_s}/3D_e$
Heat transfer parameters	
Thermicity parameter	$\beta_1 = \dfrac{(-\Delta H)B_{l_i}}{T_0 C_{p_l} \rho_l \,(1 + [U_g C_{p_g} \rho_g / U_l C_{p_l} \rho_l])}$
Bed-to-wall heat transfer	$\beta_2 = \dfrac{4U_w L}{d_T C_{p_l} \rho_l (1 + [U_g C_{p_g} \rho_g / U_l C_{p_l} \rho_l])}$
Reaction rate constants	$\alpha_r = Lwk_l B_{l_i}/U_l$
Equilibrium constants	$k_{21} = k_2/k_1;\ k_{31} = k_3/k_1;\ k_{41} = k_4/k_1$ $k_b = K_B B_{l_i};\ k_c = K_C B_{l_i};\ k_e = K_E B_{l_i}$
Thiele parameter	$\phi = R/3(\rho_p k_l B_{l_i}/D_e)^{0.5} \left[\dfrac{b_1 + k_{21} b_1 + k_{31} c_1 + k_{41} c_1}{1 + k_b b_l + k_c c_l + k_e e_l} \right]^{0.5}$
Dimensionless constant characterestic of stagnant zone	$\alpha_s = (k_{ex} \varepsilon_{l_s} / f_s k_{s_s} a_p)$

we also have

$$f_d k_{s_d} a_p (A_{l_d} - A_{s_d}) = \frac{f_d \eta_c W (k_1 B_l + k_2 B_l + k_3 C_l + k_4 E_l) A_{s_d}}{(1 + K_B B_l + K_C C_l + K_E E_l)}. \quad (13)$$

In the stagnant zone we have

$$K_{ex} \varepsilon_{ls} (A_{l_d} - A_{l_s}) = f_s k_{s_s} a_p (A_{l_s} - A_{s_s}) = \frac{f_s \eta_c W (k_1 B_l + k_2 B_l + k_3 C_l + k_4 E_l) A_{s_s}}{(1 + K_B B_l + K_C C_l + K_E E_l)} \quad (14)$$

The liquid entering the stagnant zone from the dynamic zone, characterized by the volumetric mass exchange coefficient, K_{ex}, containing the dissolved gaseous species A, at steady state is in equilibrium with liquid–solid mass transfer term in the stagnant zone and the reaction in the catalyst particles in the stagnant zones (including pore diffusion effects).

The mass balance for species A in the dry zone is

$$(1 - f_d - f_s) k_{s_g} a_p (A^* - A_{s_g}) = \frac{(1 - f_d - f_s) \eta_c W (k_1 B_l + k_2 B_l + k_3 C_l + k_4 E_l) A_{s_g}}{(1 + K_B B_l + K_C C_l + K_E E_l)} \quad (15)$$

Equations (12)–(15) can be simplified and expressed in terms of dimensionless parameters. The unknown surface concentrations can be suitably expressed in terms of known parameters (see Appendix A). The final mass balance equations in dimensionless form for species A are given as

$$-\frac{da_{l_d}}{dz} + \alpha_{gl}(1 - a_{l_d}) = \frac{\eta_c \alpha_r (b_l + k_{21} b_l + k_{31} c_l + k_{41} e_l)}{(1 + k_b b_l + k_c c_l + k_e e_l)} \times \left\{ \frac{f_d a_{l_d}}{(1 + \eta_c \phi^2 / N_d)} + \frac{f_s a_{l_d}}{[(1 + \eta_c \phi^2 / N_s) + (\eta_c \phi^2 / \alpha_s N_s)]} \right\} \quad (16)$$

$$(1 - f_d - f_s) \alpha_{gs} (1 - a_{s_g}) = (1 - f_d - f_s) \times \frac{\eta_c \alpha_r (b_l + k_{21} b_l + k_{31} c_l + k_{41} e_l)}{(1 + k_b b_l + k_c c_l + k_e e_l)} \times \left[\frac{1}{(1 + \eta_c \phi^2 / N_g)} \right]. \quad (17)$$

Similarly, the mass balances of liquid-phase reactants/products in dimensionless form can be given as

$$-\frac{db_{l_d}}{dz} = \frac{\eta_c \alpha_r (b_l + k_{21} b_l)}{q_B (1 + k_b b_l + k_c c_l + k_e e_l)} \times \left\{ \frac{f_d a_{l_d}}{(1 + \eta_c \phi^2 / N_d)} + \frac{f_s a_{l_d}}{[(1 + \eta_c \phi^2 / N_s) + (\eta_c \phi^2 / \alpha_s N_s)]} + \frac{1}{(1 + \eta_c \phi^2 / N_g)} \right\} \quad (18)$$

$$\frac{dc_{l_d}}{dz} = \frac{\eta_c \alpha_r (b_l - k_{31} c_l)}{q_B (1 + k_b b_l + k_c c_l + k_e e_l)} \times \left\{ \frac{f_d a_{l_d}}{(1 + \eta_c \phi^2 / N_d)} + \frac{f_s a_{l_d}}{(1 + \eta_c \phi^2 / N_s) + (\eta_c \phi^2 / \alpha_s N_s)]} + \frac{1}{(1 + \eta_c \phi^2 / N_g)} \right\} \quad (19)$$

$$\frac{de_{l_d}}{dz} = \frac{\eta_c \alpha_r (k_{21} b_l - k_{41} e_l)}{q_B (1 + k_b b_l + k_c c_l + k_e e_l)} \times \left\{ \frac{f_d a_{l_d}}{(1 + \eta_c \phi^2 / N_d)} + \frac{f_s a_{l_d}}{[(1 + \eta_c \phi^2 / N_s) + (\eta_c \phi^2 / \alpha_s N_s)]} + \frac{1}{(1 + \eta_c \phi^2 / N_g)} \right\} \quad (20)$$

$$\frac{dp_{l_d}}{dz} = \frac{\eta_c \alpha_r (k_{31} c_l + k_{41} e_l)}{q_B (1 + k_b b_l + k_c c_l + k_e e_l)} \times \left\{ \frac{f_d a_{l_d}}{(1 + \eta_c \phi^2 / N_d)} + \frac{f_s a_{l_d}}{[(1 + \eta_c \phi^2 / N_s) + (\eta_c \phi^2 / \alpha_s N_s)]} + \frac{1}{(1 + \eta_c \phi^2 / N_g)} \right\} \quad (21)$$

Lastly, in deriving a non-isothermal trickle-bed reactor model, the dependencies of various parameters like, reaction rate constants, equilibrium constants, effective diffusivity and saturation solubility on temperature are accounted for. The change in rate and equilibrium constants with respect to temperature can be represented as

$$k_i(T) = k_i(T_0) \exp\left[\frac{E_i}{RT_0} \left(1 - \frac{1}{\theta} \right) \right] \quad (22)$$

$$K_i(T) = K_i(T_0) \exp\left[\frac{-\Delta H_i}{RT_0} \left(1 - \frac{1}{\theta} \right) \right] \quad (23)$$

where $\theta = T/T_0$. The variation of effective diffusivity with respect to temperature can be expressed as

$$D_e(T) = D_e(T_0)\exp\left[\frac{E_D}{RT_0}\left(1 - \frac{1}{\theta}\right)\right] \quad (24)$$

where

$$D_e(T_0) = D_m\frac{\varepsilon}{\tau}. \quad (25)$$

Here D_m is the molecular diffusivity and is evaluated from the correlation of Wilke and Chang (1955). ε and τ represent the porosity and the tortuosity factors (see Table 2). The dependence of saturation solubility on temperature is given as

$$(A^*)_T = [P - (P_V)_T][(H_e)_T] \quad (26)$$

where P_V is the change in vapour pressure of the solvent due to temperature rise, given as

$$\log(P_V)_T = \frac{0.2185 \times 8365.2}{T} + 8.00117. \quad (27)$$

H_e is the Henry's law constant, expressed as

$$(H_e)_T = 1.275 \times 10^{-5} + 5.58 \times 10^{-8} \times T. \quad (28)$$

The above equations [eqs (26)–(28)] are applicable when ethyl acetate is used as a solvent (Stephen and Stephen, 1963; Weast and Astle, 1976). Owing to the exothermicity of the reaction, an increase in the bed temperature is expected and as a consequence might lead to enhanced rates. The heat generated within the reactor is mainly carried away by the flowing liquid and also due to transfer of heat from the catalyst particle to the reactor wall which is characterized by the bed to wall heat transfer coefficient, U_W. Under such conditions, where the interphase and intraparticle heat transfer resistances are assumed to be negligible, the heat balance of the reactor can be given as (Ramachandran and Chaudhari, 1983)

$$(U_l C_{p_l}\rho_l + U_g C_{p_g}\rho_g)\frac{dT}{dx} = \frac{(-\Delta H)\eta_c\alpha_r(b_l + k_{21}b_l + k_{31}c_l + k_{41}e_l)}{q_B(1 + k_b b_l + k_c c_l + k_e e_l)} \times \left\{\frac{f_d a_{l_d}}{(1 + \eta_c\phi^2/N_d)} + \frac{f_s a_{l_d}}{[(1 + \eta_c\phi^2/N_s) + (\eta_c\phi^2/\alpha_s N_s)]} + \frac{1}{(1 + \eta_c\phi^2/N_g)}\right\} - \frac{4U_W(T_b - T_W)}{d_T}. \quad (29)$$

The above equation in dimensionless form can be written as

$$\frac{d\theta}{dz} = \frac{3\eta_c\alpha_r\beta_2(b_l + k_{21}b_l + k_{31}c_l + k_{41}e_l)}{q_B(1 + k_b b_l + k_c c_l + k_e e_l)} \times \left\{\frac{f_d a_{l_d}}{(1 + \eta_c\phi^2/N_d)} + \frac{f_s a_{l_d}}{[(1 + \eta_c\phi^2/N_s) + (\eta_c\phi^2/\alpha_s N_s)]} + \frac{1}{(1 + \eta_c\phi^2/N_g)}\right\} 1 - \beta_2(\theta_b - \theta_W) \quad (30)$$

where β_2 is the thermicity parameter. Equation (30) can be used to predict the maximum temperature rise along the length of the reactor. The various dimensionless parameters in the above model are given in Table 5. Equations (16)–(21) combined with eq. (30) were solved using a fourth-order Runge–Kutta method with the following initial conditions:

$$\text{at } z = 0, a_l = b_l = 1; \quad c_l = e_l = p_l = 0; \quad \theta = 1. \quad (31)$$

This model allows prediction of the concentration of reactants/products and the temperature profile along the length of the reactor. Thus, at any given length of the reactor the (fractional) conversion of DNT (X_B) is calculated as

$$X_B = 1 - b_l. \quad (32)$$

The overall rate of hydrogenation is calculated as

$$R_A = \frac{U_l}{L}(3C_l + 3E_l + 6P_l). \quad (33)$$

Here, U_l, is the liquid velocity in m/s, L is the length of the catalyst bed in m, C_l, E_l, P_l, are the concentrations of 4A2NT, 2A4NT and TDA, respectively, in kmol/m^3. The selectivity to TDA (S_{TDA}) is calculated as

$$S_{TDA} = \frac{p_l}{(1 - b_l)} \times 100. \quad (34)$$

and the maximum temperature rise is calculated as

$$(\Delta T_{max}) = T - T_0 \quad (35)$$

where T represents the actual temperature calculated from eq. (30) and T_0 represents the initial temperature. When calculations are performed for $z = 1$, we get the above quantities for the entire reactor.

RESULTS AND DISCUSSION

The model equations developed in the earlier section allow prediction of the conversion of DNT (X_B), global rate of hydrogenation (R_A), selectivity to TDA and the maximum temperature rise (ΔT_{max}) for a given set of inlet conditions in a trickle-bed reactor. In order to predict the performance behaviour from this mathematical model developed, a knowledge of kinetics, mass and heat transfer parameters and hydrodynamic parameters is most essential. The rate parameters used are given in Table 3. For gas–liquid and liquid–solid mass transfer coefficients and overall heat transfer coefficient, correlations summarized in Table 6 were used. The details of these are discussed below.

As indicated earlier, the model proposed here is applicable for conditions of complete wetting of the

Table 6. Summary of various correlations used in this work

Parameter	Author's name (Year)
Gas–liquid mass transfer coefficient	Goto and Smith, (1975)
Liquid–solid mass transfer coefficient	Satterfield *et al.* (1978)
Gas-particle mass transfer coefficient (value used)	2.5×10^{-6} m/s; Zheng Lu *et al.* (1984)
Volumetric mass exchange coefficient	Hochmann and Effron (1969)
Total liquid hold-up	Sato *et al.*, (1973)
Static liquid hold-up (value used)	0.05, Zai-sha Mao *et al.* (1993)
Molecular diffusivity	Wilke and Chang (1955)
Saturation solubility	Stephen and Stephen, (1963) and Weast and Astle (1976)
Bed-to-wall heat transfer coefficient	Baldi (1981)
Wetting efficiency	Mills and Dudukovic (1981)

catalyst particles ($f_d = 1$, $f_s = 0$), partial wetting of the catalyst particles ($f_d < 1$, $f_s = 0$) and when there are significant stagnant liquid pockets ($f_d < 1, f_s < f_d$). In order to evaluate the wetted fractions in the two zones (dynamic and static) separately, as a first approximation we have assumed that the ratio of the wetted fractions of dynamic and static zones is proportional to their respective liquid hold-ups, i.e.

$$\left(\frac{f_d}{f_s}\right) = \left(\frac{\varepsilon_d}{\varepsilon_{ls}}\right). \tag{36}$$

On the other hand, the sum of the two wetted fractions ($f_d + f_s = f_w$) is equal to the total wetted fraction f_w. Also, the total liquid hold-up ε_l is equal to the stagnant liquid hold-up, ε_{ls} and the dynamic liquid hold-up, ε_{ld}, i.e. ($\varepsilon_l = \varepsilon_{ls} + \varepsilon_{ld}$). There is very limited information available on stagnant liquid hold-up, ε_{ls}; however, Zai-Sha *et al.* (1993) reported experimental data from which ε_{ls}, was found to be 0.05. The total liquid hold-up, ε_l, was evaluated from the correlation proposed by Sato *et al.* (1973). The dynamic liquid hold-up (ε_{ld}) can be evaluated from the difference between the total liquid hold-up (ε_l) and static liquid hold-up (ε_{ls}). Thus, the wetted fraction f_s and f_d are given as

$$f_d = \frac{f_w}{(1 + \varepsilon_{ls}/\varepsilon_{ld})} \tag{37}$$

$$f_s = f_w - f_d. \tag{38}$$

Equations (37) and (38) indicate that with a knowledge of the total wetted fraction, and from the dynamic and static liquid hold-ups it would be possible to calculate the wetted fractions in the two zones separately. The total wetted fraction was calculated by the following correlation proposed by Mills and Dudukovic (1981) under our reaction conditions:

$$f_w = 1 - \exp\left(-1.35\, Re_l^{0.333}\, We_l^{0.17} \times \left(\frac{a_t d_p}{\varepsilon_b^2}\right)^{0.0425}\right). \tag{39}$$

As the liquid velocity increased from 1×10^{-5} to 2×10^{-4} m/s, the wetted fraction increased from 0.2 to 0.6 indicating that even at a liquid velocity of 2×10^{-4} m/s around 40% of the catalyst surface remains exposed to the gas directly.

The gas–liquid and liquid–solid mass transfer coefficients were evaluated from the correlations of Goto and Smith (1975) and Satterfield *et al.* (1978), respectively. For a gas–liquid–solid reaction in a trickle-bed reactor under conditions of stagnant liquid pockets, it has been shown by Sicardi *et al.* (1980) and Colombo *et al.* (1976) that the liquid–solid mass transfer in the stagnant zone can be as much as 20–100 times less than the liquid–solid mass transfer in the dynamic zone and as much as 20–30% of the total area of the catalyst can be covered by stagnant zones under certain conditions. For the present study, as a first step, the ratio of liquid–solid mass transfer in dynamic zone to stagnant zone was assumed to be equal to 20. Also, under conditions of partial wetting a third mass transfer term, the gas–solid mass transfer resistance needs to be incorporated. Zheng Lu *et al.* (1984) reported some data on gas-particle mass transfer coefficient, but the data are very limited and therefore, in our work k_{gs} values were obtained by fitting the observed experimental data for some conditions. The k_{gs} value thus obtained was 2.5×10^{-6} m/s. For all further calculations this value has been used. The k_{gs} value reported in this work is slightly on the lower side when compared to the value reported by Zheng Lu *et al.* (1984). Uncertainty in this value exists as there are no literature correlations proposed for evaluating the gas-particle mass transfer coefficient. The other parameters that are required are the volumetric mass exchange coefficient K_{ex} and the bed-to-wall heat transfer coefficient. The correlation proposed by Hochmann and Effron (1969) was used to calculate the volumetric mass exchange coefficient

$$K_{ex} = 0.01 Re_l^{0.6}. \tag{40}$$

The above equation assumes that the hold-up consists of liquid and stagnant pockets that exchanges mass slowly or irregularly with an active fraction of the

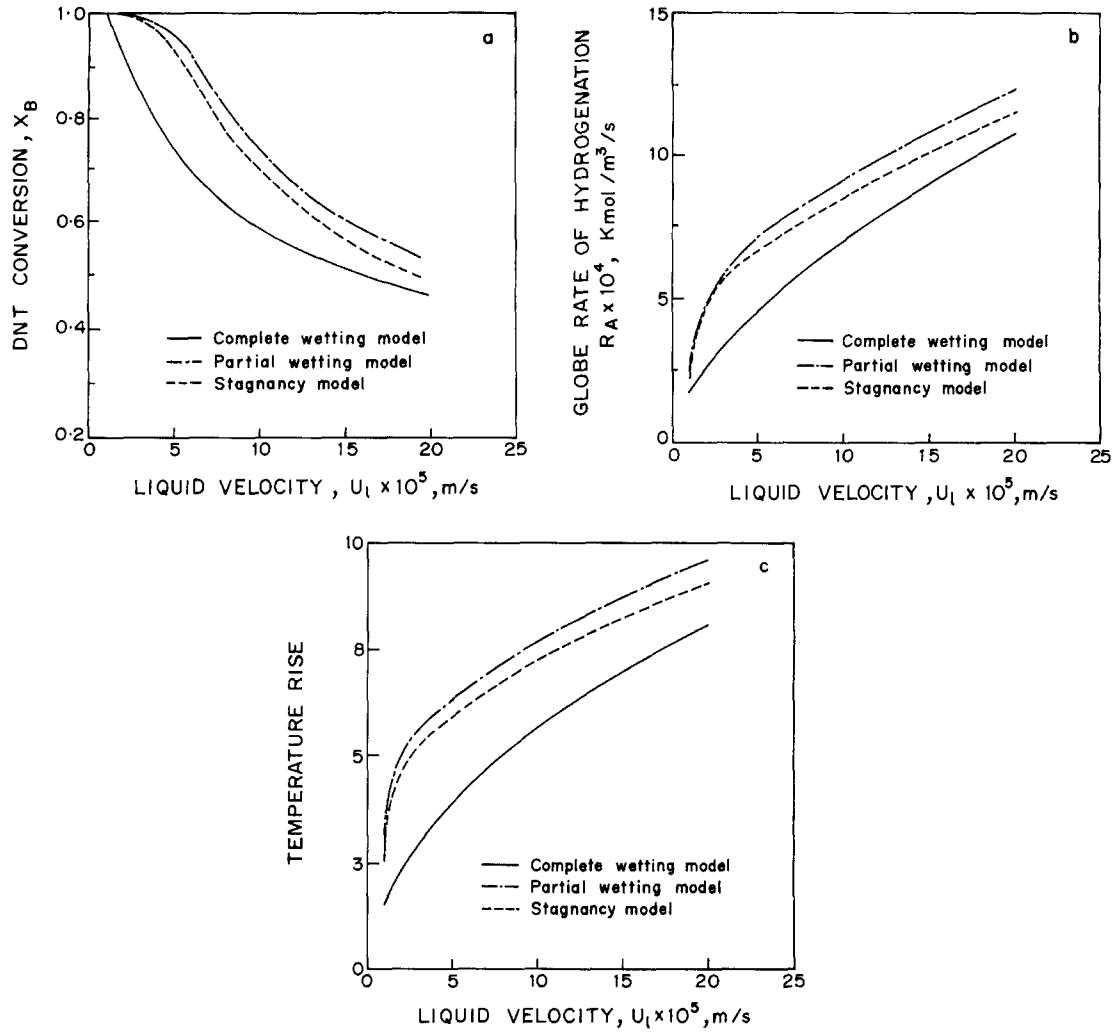

Fig. 4. (a)–(c) show model predictions of DNT conversion, global hydrogenation rates and temperature rise with liquid velocity at 363 K. Initial conditions: $B_{l_i} = 0.2$ kmol/m^3; H_2 pressure: 1.4 MPa; $U_g = 4.23 \times 10^3$ m/s; temperature = 363 K.

liquid moving in plug flow. The overall bed-to-wall heat transfer coefficient, U_w, was evaluated from the following correlation proposed by Baldi (1981) for low interaction regime:

$$\frac{U_w d_p}{\lambda_{eff}} = 0.057\left(\frac{U_l \rho_l d_p}{\varepsilon_l \mu_l}\right)^{0.89} (Pr)^{1/3}. \qquad (41)$$

Using the above correlations and the kinetic parameters given in Table 3, the performance of the trickle-bed reactor under non-isothermal conditions was predicted theoretically to understand the significance of different parameters. Typical results of conversion of DNT (X_B), global rate of reaction (R_A) and maximum temperature rise, ΔT_{max}, at 363 K are shown in Fig. 4. The model predictions at complete wetting of catalyst particles, partial wetting of catalyst particles and in the presence of significant stagnant liquid pockets are presented. As the liquid velocity varied from 1×10^{-5} to 2×10^{-4} m/s, the conversion varied from nearly 100 to 55% for partial wetting as well as the stagnancy model [Fig. 4(a)]. However, the conversions predicted by the complete wetting model were significantly lower at low liquid velocities. Only at very high liquid velocities, the difference in conversion levels predicted among the three models reduced substantially as expected. The global rates of hydrogenation shown in Fig. 4(b) indicate a similar trend. In the case of the partial wetting model and stagnancy model the global rates increase steeply at lower liquid velocities unlike the case with complete wetting model, wherein the predicted rates are much lower and increase steadily. In all the three cases the global rate of hydrogenation increases with increasing liquid velocity. Figure 4(c) shows the maximum temperature rise, ΔT_{max} at 363 K. For this set of initial conditions, the maximum temperature rise, ΔT_{max}, was found to be around 10 K at higher velocities. Also, the ΔT_{max} predicted by the complete wetting model is lower than the ΔT_{max} predicted by the partial wetting and

stagnancy models. In this case also, a steep rise in the maximum temperature rise, ΔT_{max}, was observed at lower velocities. Similar trends were observed for the reaction at 343 K. For the present set of conditions and the liquid velocities in the range shown in Figs 4, the wetted fractions varied approximately from 0.2 to 0.6 indicating that there is every possibility for the catalyst particle to interact directly with the gas phase. As the gas diffusion is several orders of magnitude higher when compared to that in the liquid, under conditions of partial wetting, it is expected to show a higher rate of reaction. At very low liquid velocities, a significant fraction of the catalyst particles remains unwetted and hence for the partial wetting, higher rates and higher conversion levels are observed. As a consequence, depending on the exothermicity of the reaction the maximum temperature rise (ΔT_{max}) is also increased. For complete wetting model, the gas–liquid and liquid–solid mass transfer limitations influence the overall rate, which is substantially eliminated in partially wetted conditions to facilitate direct gas–particle mass transfer. This is consistent with the observed trends for these models. At very high liquid velocities, the catalyst particles become more and more wetted externally and, hence, the conversion levels predicted by the three models agree. One more important conclusion from Fig. 4 is that the global rates, conversion and the maximum temperature rise predicted by the stagnancy model differ only marginally when compared with the partial wetting model. Also we can see that in all the cases the performance behaviour predicted by the stagnancy model is always less than that predicted by partial wetting model. While this decrease in performance can be attributed to the liquid–solid mass transfer term in the stagnant zone being several times less than the corresponding term in the dynamic zone, it is important to quantitatively analyse the role of stagnancy at this point.

In order to understand the role of stagnancy on the performance of a trickle-bed reactor, it is necessary to predict the global reaction rates as a function of the parameters that contribute to the effect of stagnant liquid hold-up. For this purpose, the global reaction rates were plotted as a function of the ratio of the liquid hold-ups in the static and dynamic zones ($\varepsilon_{ls}/\varepsilon_{ld}$) as shown in Fig. 5. Even when 30% of the catalyst particle was exposed to stagnant liquid, there was no significant change in the global rates (< 5% decrease) in the reaction rates indicating that for all practical purposes applicable to hydrogenation of DNT in a trickle-bed reactor, the role of stagnancy is unimportant for conditions described in this work. This quantitative analysis on the role of stagnancy is important for the present case, as it was predicted by many authors that stagnancy might play a major role in the performance of a trickle-bed reactor (Sicardi *et al.*, 1980; Colombo *et al.*, 1976; Chaudhari and Ramachandran, 1992) under conditions of liquid–solid mass transfer and intraparticle diffusional limitations.

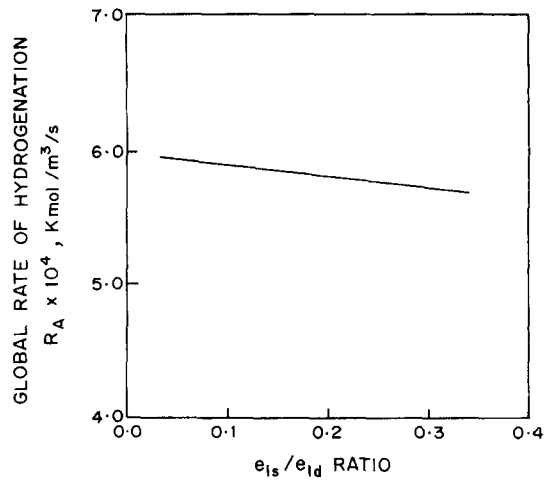

Fig. 5. Effect of stagnancy on the global rate of hydrogenation at 343 K. Initial conditions: $B_{l_i} = 0.2$ kmol/m^3; H_2 pressure: 1.4 MPa; $U_g = 4.23 \times 10^{-3}$ m/s; temperature = 343 K, $U_l = 7.5 \times 10^{-5}$ m/s.

In order to understand the sensitivity of the model with respect to the gas–liquid mass transfer resistance, the gas–liquid mass transfer coefficient obtained from the correlation of Goto and Smith (1975) for the present case, was increased and decreased by 10 times. The results are shown in Fig. 6, plot (d). An increase in the mass transfer coefficient by 10 times increases the reaction rates substantially at liquid velocities greater than 5×10^{-5} m/s. The global rates were found to be greater than twice when $k_l a_B$ value was increased by 10 times. Also, when the $k_l a_B$ value was decreased by 10 times, the global rates reduced by approximately 50% over the entire range of liquid velocity studied. This is a clear indication that the gas–liquid mass transfer resistance is significant. The effect of liquid–solid mass transfer on the global rate is shown in plot (e) of Fig. 6. In this case, the liquid–solid mass transfer coefficient was predicted from the correlation of Satterfield *et al.* (1978). The results indicate that the influence of liquid–solid mass transfer on the global rate of hydrogenation is also significant. When the k_s value was increased by 10 times the global rates increased by approximately 30% after a liquid velocity of 5×10^{-5} m/s. This difference in global rates was maintained over the entire range of liquid velocity investigated. However, a decrease in the value of k_s by 10 times reduced substantially the global rates (the rates reduced by more than a factor of 2). The sensitivity of the model with respect to the gas-particle mass transfer coefficient is shown in plot (f). The value used in this work is 2.5×10^{-6} m/s. Figure 6(f) is obtained by increasing and decreasing this value of k_{gs} by 2 times. As can be seen, by increasing this value just by 2 times the global rates increase by approximately 30% after a certain liquid velocity (5×10^{-5}, m/s), since in this case an increased contribution is through the dry zone. The conversions though not shown here increased substantially from 40 to 50% at the highest liquid velocity (2×10^{-4} m/s). Thus, the

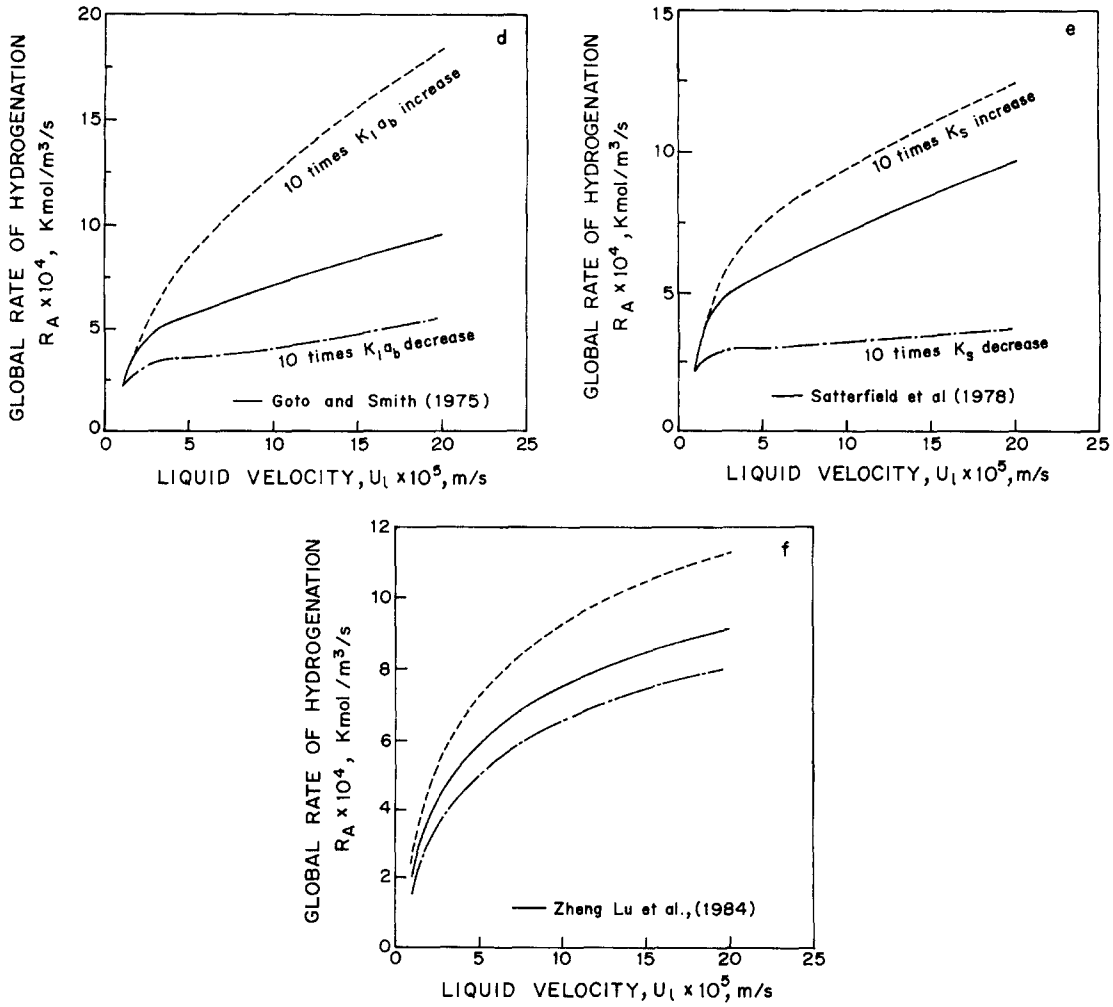

Fig. 6. (d)–(f) show the sensitivity of the model with respect to gas–liquid, liquid–solid and gas–solid mass transfer resistances at 343 K. Initial conditions: $B_{l_i} = 0.2$ kmol/m^3; H_2 pressure: 1.4 MPa; $U_g = 4.23 \times 10^{-3}$ m/s; temperature = 343 K.

relative importance of the mass transfer resistances in decreasing order as predicted by the trickle-bed reactor model applicable to hydrogenation of DNT can be given as gas–solid, k_{gs} > gas–liquid, $k_l a_b \simeq$ liquid–solid k_s.

Experimental results and comparison with model predictions

In this section, experimental results on hydrogenation of DNT in a trickle-bed reactor are compared with model predictions. Experiments were performed with varying liquid velocity at 318 and 328 K to obtain DNT conversion, global rates of hydrogenation and the maximum temperature rise. Experiments were also performed in order to understand the effect of gas velocity at a constant liquid velocity of 1.5×10^{-4} m/s and the effect of particle size (for understanding intraparticle diffusion effects). In all the above experiments, the various products formed during the hydrogenation of DNT were found to be 2-amino-4-nitrotoluene (2A4NT), 4-amino-2-nitrotoluene (4A2NT) and 2,4 toluenediamine (TDA). The progress of the reaction is well represented by the reaction scheme shown in Fig. 2.

Before we go into the detailed analysis and comparison of the experimental results with the model predictions, it is necessary to justify the various assumptions made in deriving the model applicable for hydrogenation of DNT. For this purpose, several diagnostic criteria proposed in the literature were used. By using the criteria proposed by Mears (1971), it was established that the liquid was in plug flow and the intraparticle and interphase temperature gradients were negligible. The criteria of Lee and Smith were used to confirm that the catalyst particles were partially wetted and the wetted fraction was calculated using eq. (39).

In order to verify the applicability of the model, several experiments were done and the results are compared with the model predictions. Here, it should be noted that the experimental results are compared with the complete wetting model and the partial

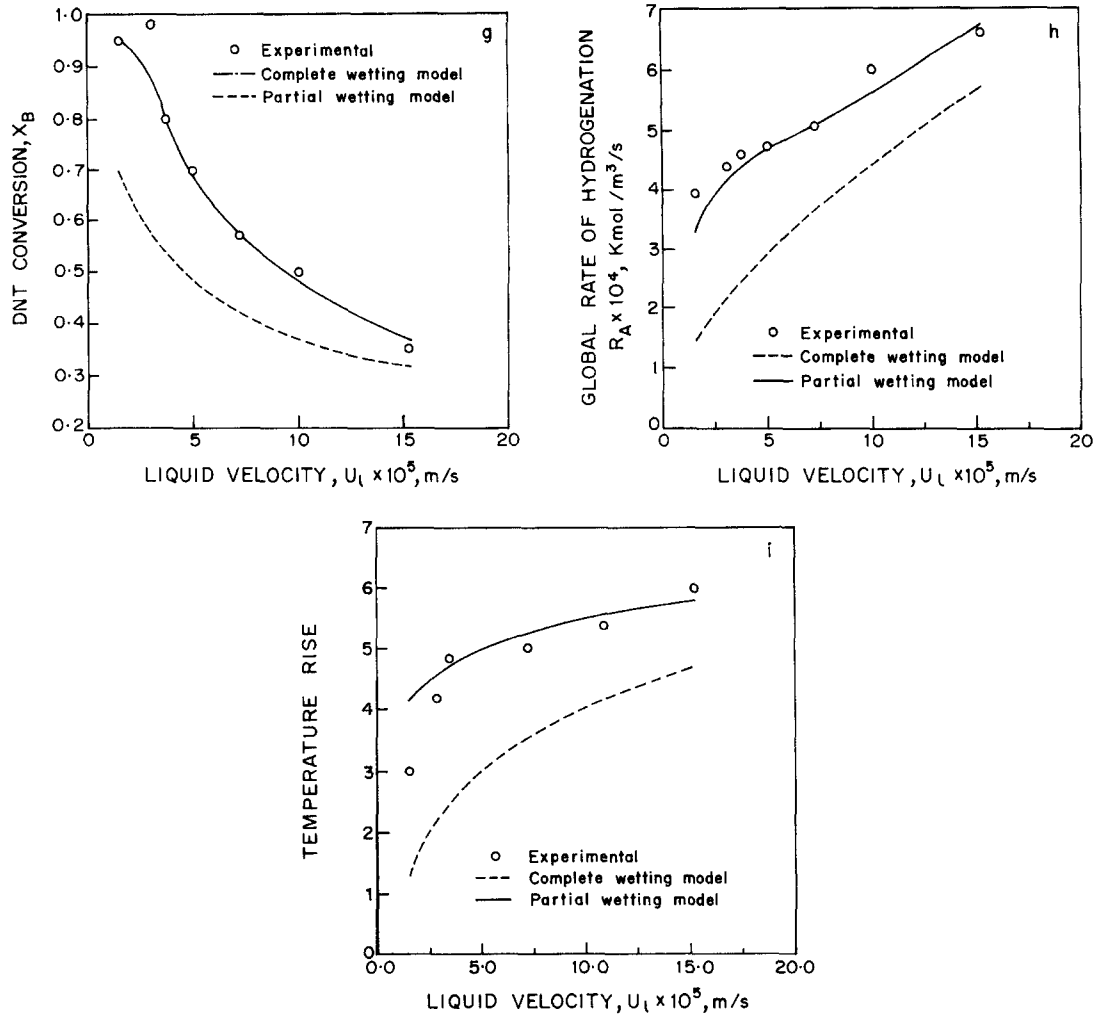

Fig. 7. (g)–(i) show comparison between experimental observations and model predictions with respect to DNT conversion, global hydrogenation rates and temperature rise vs liquid velocity at 318 K. Initial conditions: $B_{l_i} = 0.2$ kmol/m^3; H_2 pressure: 1.4 MPa; $U_g = 4.23 \times 10^{-3}$ m/s; temperature = 318 K.

wetting model as we have earlier demonstrated theoretically that stagnancy is unimportant for the present case. Figure 7 shows three plots wherein experimental data obtained as a function of liquid velocity at 318 K (shown as open circles) was compared with model predictions. Plot (g) represents the conversion of DNT, plot (h) represents the global rate of hydrogenation and plot (i) represents the maximum temperature rise. In all cases it can be seen that the experimental data match with the partial wetting model (exceptions being the conversion of DNT at liquid velocity of 3×10^{-5} m/s and the maximum temperature rise data at a liquid velocity of 1.5×10^{-5} m/s which would have arised due to a possible experimental error rather than the inadequacy of the model). On the other hand, complete wetting model underpredicts the reactor performance, especially at lower liquid velocities ($< 1 \times 10^{-4}$ m/s). At higher liquid velocities ($> 1 \times 10^{-4}$ m/s) the wetted fraction of the catalyst particle increases and as a consequence the predictions of complete wetting model are also closer to the experimental observations (atleast with respect to the DNT conversion, though not really for the global rates and temperature rise). Hence, at this stage it is appropriate to comment that partial wetting model explains the experimental observations reasonably well. The effect of gas velocity (at a constant liquid velocity of 1.5×10^{-4} m/s) on the global rate of hydrogenation is shown in Fig. 8. The results indicate that the effect of gas velocity is negligible. Such type of negligible influence of gas velocity has earlier been observed by Goto and Smith (1975) for formic acid oxidation. As the gas is only sparingly soluble, the variation in gas velocity would have only slightly influenced the gas–liquid mass transfer coefficient in the dynamic zone and hence we do not observe any dependence. Figure 9 shows the influence of the particle size on the global rate of hydrogenation. Experimental results at two different particle sizes (1×10^{-3} and 2×10^{-3} m) were compared with the partial wetting model. The results indicate that the reaction is severely diffusion controlled. This influence of

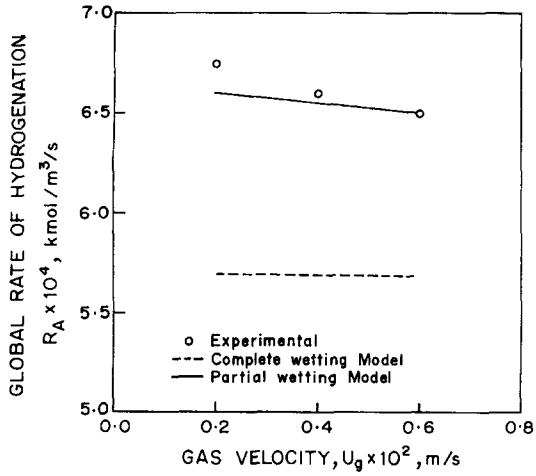

Fig. 8. Effect of gas velocity on the global rate of hydrogenation at 318 K. Initial conditions: $B_{l_i} = 0.2$ kmol/m^3; H_2 pressure: 1.4 MPa; $U_l = 1.5 \times 10^{-4}$ m/s; temperature = 318 K.

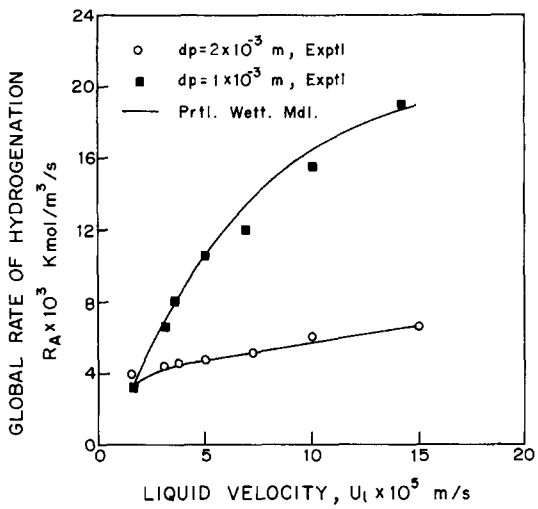

Fig. 9. Effect of particle size (d_p) on the global rate of hydrogenation at 318 K. Initial conditions: $B_{l_i} = 0.2$ kmol/m^3; H_2 pressure: 1.4 MPa; $U_g = 4.23 \times 10^{-3}$ m/s; temperature = 318 K.

intraparticle diffusion seems to be more predominant when compared with the influence of external mass transfer resistances. Experimental data obtained at 318 and 328 K was compared with the model predictions and the results are shown in Fig. 10. A good agreement between the model predictions and the data obtained at two different temperatures is observed. Thus, the partial wetting model represents the experimental data for a wide range of operating conditions satisfactorily.

Finally, in order to understand the multiplicity phenomenon and hysteresis behaviour in a trickle-bed reactor and to investigate the heat effects, several experiments were carried out at initial conditions (DNT concentration = 0.5 kmol/m^3, H_2 pressure = 3 MPa and temperature = 328 K) such that ΔT_{max}

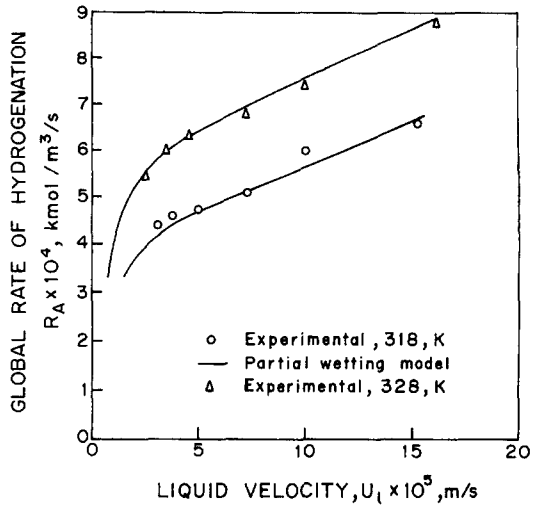

Fig. 10. Effect of temperature on the global rate of hydrogenation. Initial conditions: $B_{l_i} = 0.2$ kmol/m^3; H_2 pressure: 1.4 MPa; $U_g = 4.23 \times 10^{-3}$ m/s.

is significant. These results are shown in Fig. 11. Unlike the experiments discussed earlier, this experiment was carried out initially with increasing liquid velocity after which the liquid velocity was reversed keeping all other conditions same. For each liquid velocity, the conversion of DNT, global rates of hydrogenation and the selectivity towards TDA were observed along with maximum temperature rise due to the high exothermicity of the reaction ($-\Delta H = 556$ kJ/mol of nitro group). The temperature in catalyst bed drastically increased with increase in the liquid velocity as shown in plot (j) of Fig. 11. A temperature rise (ΔT_{max}) of 35 K was observed for a liquid velocity of 4.5×10^{-4} m/s. The reversal of the liquid velocity however did not follow the same path. The catalyst bed was found to be at a much higher temperature in the decreasing mode of operation over the entire range of liquid velocity investigated. This influenced the conversion of DNT and more predominantly the selectivity towards TDA as shown in plots (L) and (m) of Fig 12. The conversion levels increased by 10% for the entire range of liquid velocities in the second mode of operation and the selectivity difference towards TDA was around 25% at a liquid velocity of 1×10^{-4} m/s. Such a behaviour is expected for exothermic reactions in a trickle-bed reactor, wherein the conditions prior to each variation are not the same with respect to temperature of catalyst bed. Hence, the multiplicity of conversion, global rates and TDA selectivity as shown in Fig. 12 is observed.

CONCLUSIONS

An experimental study on hydrogenation of DNT in a trickle-bed reactor has been reported and the effect of liquid velocity, gas velocity, particle size and temperature on the conversion, global rate of hydrogenation and TDA selectivity are discussed.

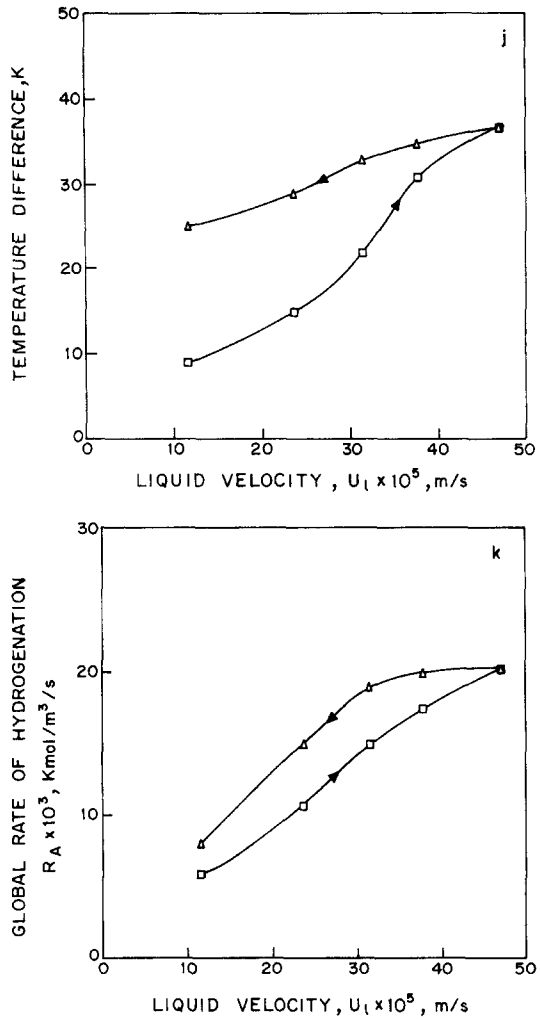

Fig. 11. (j)–(m) show experimental observations of multiplicity with respect to temperature rise, global rate of hydrogenation, DNT conversion and selectivity to TDA as a function of liquid velocity. Initial conditions: $B_{l_i} = 0.5$ kmol/m^3; H_2 pressure: 3 MPa; $U_g = 4.23 \times 10^{-3}$ m/s; temperature = 328 K.

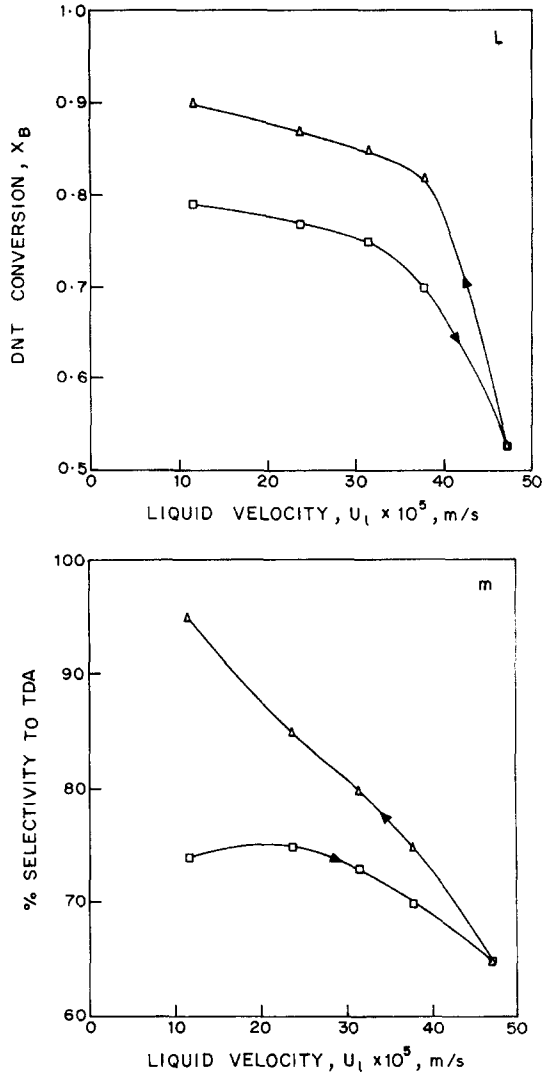

Fig. 12.

This reaction represents a complex consecutive/parallel reaction scheme with high exothermicity and the trickle-bed reactor model developed incorporates the contributions of partial wetting and stagnant liquid hold-up effects in addition to external and intraparticle mass transfer effects and heat effects. The influence of temperature on different parameters has been incorporated in order to derive a non-isothermal model. The performance of the reactor (conversion of DNT, global rate of hydrogenation and maximum temperature rise) under conditions of complete wetting of catalyst particles, partial wetting of catalyst particles and in the presence of stagnant liquid pockets in between the catalyst particles was compared theoretically. It was observed that for conditions relevant to hydrogenation of DNT, the contribution of stagnant liquid hold-up is not very significant (5–10%). However, for partially wetted catalyst particles a significant rate enhancement is observed. The sensitivity of the model with respect to external mass transfer resistances was studied theoretically and the results indicated that the relative importance of these parameters in decending order was found to be: gas-particle k_{gs} > gas–liquid, $k_l a_B$ > liquid–solid k_s. However, intraparticle diffusion resistances was found to be the major controlling resistance as predicted by the model and also consistent with the experimental data obtained for different particle sizes. The experimental data over a wide range of conditions have been compared with the model predictions. For this purpose, most of the parameters were evaluated using literature correlations. The various assumptions made in deriving the trickle-bed reactor model applicable to hydrogenation of DNT have been justified using several criteria proposed in the literature. Since, the current status of information on the gas-particle mass transfer coefficient, k_{gs}, (required for predicting the reactor performance under conditions of partial wetting of catalyst particles) is very limited, this parameter was estimated

by simulating the experimental data for certain set of inlet conditions. This value was found to be 2.5×10^{-6} m/s which was used in all other calculations at different conditions. A comparison of experimental data with theoretical predictions showed excellent agreement for partial wetting model, indicating that the unwetted fraction of the catalyst particle was in the range 0.2–0.6 as calculated from the correlations of Mills and Dudukovic (1981) for the conditions used in this work. Thus, the model proposed here was found to be representative over a wide range of operating conditions.

Acknowledgement

MVR wishes to thank Council of Scientific and Industrial Research (CSIR), India, for providing him a Research Fellowship.

NOTATIONS

a_l concentration of hydrogen in liquid phase, $(= A_l/A^*)$, dimensionless

a_s concentration of hydrogen on the catalyst surface, $(= A_s/A^*)$, dimensionless

a_p external surface area of the pellet $[= 6(1 - \varepsilon_B)/d_p]$, m^{-1}

a_t packing external surface area of the per unit volume of reactor $[= S_{ex}(1 - \varepsilon_b)/V_B]$, m^{-1}

a_w catalyst area wetted, m^{-1}

A_l concentration of hydrogen in liquid phase, kmol/m^3

A_s concentration of hydrogen on the catalyst surface, kmol/m^3

A^* concentration of hydrogen in equilibrium with liquid, kmol/m^3

b_l concentration of DNT in liquid phase $(= B_l/B_{li})$, dimensionless

B_l concentration of DNT in liquid phase, kmol/m^3

B_{li} initial concentration of DNT in liquid phase, kmol/m^3

B_{ml} liquid side Biot number $(= \varepsilon k_l P_x/D_e)$

c_l concentration of 4A2NT in liquid phase, $(= C_l/B_{li})$, dimensionless

C_l concentration of 4A2NT in liquid phase, kmol/m^3

C_{pl} heat capacity of liquid, kJ/K/kg

C_{pg} heat capacity of gas, kJ/K/kg

D_e effective diffusivity, m^2/s

D_M molecular diffusivity, m^2/s

d_p particle diameter, m

d_T reactor diameter, m

e_l concentration of 2A4NT in liquid phase, $(= E_l/B_{li})$, dimensionless

E_l concentration of 2A4NT in liquid phase, kmol/m^3

E_i activation energy for hydrogenation step i, kJ/mol

f_d fraction of catalyst wetted by the dynamic liquid

f_s fraction of catalyst wetted by the stagnant liquid

f_W wetted fraction

h gas-to-particle heat transfer coefficient, kJ/m^2/K/s

k_1 to k_4 reaction rate constants, (m^3/kg) (m^3/kmol) s^{-1}

k_{21} dimensionless rate constant $(= k_2/k_1)$

k_{31} dimensionless rate constant $(= k_3/k_1)$

k_{41} dimensionless rate constant $(= k_4/k_1)$

k_b, k_c, k_e dimensionless equilibrium constants $(k_b = K_B B_{li}; k_c = K_C B_{li}; k_e = K_E B_{li})$

k_s liquid–solid mass transfer coefficient, m s^{-1}

k_{gs} gas–particle mass transfer coefficient, m s^{-1}

K_A, K_B K_C, K_E equilibrium constants, m^3/kmol

$k_l a_B$ gas–liquid mass transfer coefficient, s^{-1}

K_{ex} exchange coefficient between dynamic and stagnant liquid, s^{-1}

L reactor length, m

L_m superficial liquid mass velocity, kg/m^2/s

n order of reaction

N_d Nusslet number for liquid phase in the dynamic zone

N_s Nusslet number for liquid phase in the stagnant zone

N_g Nusslet number for gas phase

p_l concentration of TDA in liquid phase $(= P_l/B_{li})$, dimensionless

P_l concentration of TDA in liquid phase, kmol/m^3

P_x characterstic dimension of the pellet, volume/ outer surface area

Pr Prandlt number of liquid phase $(= C_{pl}\mu_l/\lambda_{eff})$

q_B stiochiometric ratio $(= 3B_{li}/A^*)$

r_1 to r_4 reaction rate for individual hydrogenation steps, kmol/m^3/s

R radius of the pellet, m

R_A overall rate of hydrogenation, kmol/m^3/s

R_g universal gas constant, kJ/kmol/K

Re_l Reynolds number for liquid phase

S_{ex} external surface area of the catalyst pellet, m^2

T_0 initial temperature, K

T_b bulk temperature, K

T_W wall temperature, K

U_W bed-to-wall heat transfer coefficient, kJ/m^2/K/s

U_g gas velocity, m/s

U_l liquid velocity, m/s

V_R reactor volume, m^3

W weight of the catalyst, kg/m^3

We_l Weber number for liquid $(= L_m^2/\sigma_l \rho_l a_t)$

z reactor length, dimensionless

Greek letters

α_{gl} dimensionless gas–liquid mass transfer coefficient

α_{ls}	dimensionless liquid–solid mass transfer coefficient
α_r	dimensionless reaction rate constant
α_s	dimensionless exchange coefficient
b_l	thermicity parameter
β_2	dimensionless bed-to-wall heat transfer coefficient
$\delta_{l'}$	pressure drop per unit bed height with only liquid flowing, N/m^2
$\delta_{g'}$	pressure drop per unit bed height with only gas flowing, N/m^2
ΔH	heat of reaction, kJ/mol
ε	porosity of catalyst
ε_b	bed voidage
ε_l, ε_d, ε_s	liquid hold-up, total, dynamic and stagnant
η_c	overall catalytic effectiveness factor
η_d, η_s, η_g	catalytic effectivenss factor in dynamic, stagnant and dry zones
θ	temperature, dimensionless
θ_b	bed temperature, dimensionless
θ_W	wall temperature, dimensionless
μ_l	viscosity of liquid, kg/m/s
ρ_l	density of liquid, kg/m^3
ρ_g	density of gas, kg/m^3
ρ_p	density of catalyst particle, kg/m^3
σ_l	surface tension, N/m
τ	tortuosity factor
ϕ	Thiele parameter

Subscripts

d	dynamic zone
g	dry zone
s	stagnant zone

REFERENCES

Baldi, G. (1981) In *Multiphase Chemical Reactors, Vol. II Design Methods*, eds, A. E. Rodrigues, J. M. Cole and N. M. Sweed, p. 307. Sithoff and Noorldhoff, USA.

Bischoff, K. B. (1965) Effectiveness factor for general reaction rate forms. *A.I.Ch.E. J.* **11**, 351.

Brad Sims, W., Gaskey, S. W. and Luss, D. (1994) Effect of flow regime and liquid velocity on conversion in a trickle bed reactor. *Ind. Engng Chem. Res.* **33**, 2530.

Caceres, E., Puigjaner, L. and Recasens, F. (1988) A trickle bed process for hydration of isobutene to tert-butyl alchohol: a study of reactor performance. *Chem. Engng J.* **37**, 43.

Chaudhari, R. V. and Ramachandran, P. A. (1992) Mass transfer in trickle bed reactors. In *Heat and Mass Transfer in Porous Media*, eds M. Quintard, S. Aodorovic Marija, p. 633. Elsevier, Amsterdam, Netherlands.

Colombo, A. J., Baldi, G. and Sicardi, S. (1976) Solid–liquid contacting effectiveness in trickle bed reactors. *Chem. Engng Sci.* **31**, 1101.

Funk, G. A., Harold, M. P. and Ng, K. M. (1991) Experimental study of reaction in partially wetted catalyst pellet. *A.I.Ch.E. J.* **37**, 202.

Germain, A. H., Lefebvre, A. G. and L'Homme, G. A. (1974) Experimental study of a catalytic trickle bed reactor. Advances in Chemistry Series No. 133, Chemical Reaction Engineering-II, *ACS*, p. 164.

Gianetto, A. and Specchia, V. (1992) Trickle bed reactors: state of art and perspectives. *Chem. Engng Sci.* **47**, 3197.

Gliddon, B. J. and Cranfield, R. R. (1970) Gas particle heat transfer coefficients in packed beds at Reynolds number between 2 and 100. *Br. Chem. Engng* **15**, 481.

Goto, S., Lakota, A. and Levec, J. (1981) Effectiveness factors of *n*th order kinetics in trickle bed reactors. *Chem. Engng Sci.* **36**, 157.

Goto, S. and Smith, J. M. (1975) Trickle bed reactor performance Part II: reaction studies. *A.I.Ch.E. J.* **21**, 706.

Hanika, J., Sporka, V., Ruzicka, V. and Pistek, R. (1975) Qualitative observations of heat and mass transfer effects on the behaviour of trickle bed reactor. *Chem. Engng Commun.* **2**, 19.

Hanika, J., Sporka, V., Ruzicka, V. and Pistek, R. (1977) Dynamic behaviour of an adiabatic trickle bed reactor. *Chem. Engng Sci.* **32**, 525.

Hanika, J., Vosecky, V. and Ruzicka, V. (1981) Dynamic behaviour of the laboratory trickle bed reactor. *Chem. Engng J.* **21**, 108.

Harold, M. P. and Ng, K. M. (1993) Vaporization induced dewetting of a catalyst during an exothermic reaction. *Ind. Engng Chem. Res.* **32**, 2975.

Hartman, M. and Coughlin, R. W. (1972) Oxidation of SO_2 in a trickle bed reactor with carbon. *Chem. Engng Sci.* **27**, 867.

Herskowitz, M. (1985) Modelling of a trickle bed reactor: the hydrogenation of xylose to xylitol. *Chem. Engng Sci.* **40**, 1309.

Herskowitz, M. (1988) Hydrogenation of benzaldehyde to benzyl alchohol in a slurry and trickle bed reactor. *Stud. Surf. Sci. Catal.* **59**, 105.

Hertskowitz, M., Carbonell, R. G. and Smith, J. M. (1979) Effectiveness factors and mass transfer in trickle bed reactors. *A.I.Ch.E. J.* **25**, 272.

Herskowitz, M. and Mosseri, S. (1983) Global rates and reaction in trickle bed reactors: effect of gas and liquid flow rates. *Ind. Engng Chem. Fundam.* **22**, 4.

Herskowitz, M. and Smith, J. M. (1983) Trickle bed reactors: A review. *A.I.Ch.E. J.* **29**, 1.

Hochmann, J. M. and Effron, E. (1969) Two phase cocurrent downflow in packed beds. *Ind. Engng Chem. Fundam.* **8**, 63.

Janssen, H. J., Kruithof, A. J., Steghuis, G. J. and Westerterp, K. R. (1990a) Kinetics of the catalytic hydrogenation of 2,4 dinitrotoluene I: experiments, reaction scheme and catalyst activity. *Ind. Engng Chem. Res.* **29**, 754.

Janssen, H. J., Kruithof, A. J., Steghuis, G. J. and Westerterp, K. R. (1990b) Kinetics of the catalytic hydrogenation of 2,4 dinitrotoluene H: modelling of reaction rates and catalyst activity. *Ind. Engng Chem. Res.* **29**, 1822.

Janssen, H. J., Vos, H. J. and Westerterp, K. R. (1992) A mathematical model for multiple hydrogenation reactions in a continuously stirred three phase slurry reactor with an evaporating solvent. *Chem. Engng Sci.* **47**, 4191.

Koros, R. M. (1986) Engineering aspects of trickle bed reactors. In *Chemical Reactor Design and Technology*, ed. H. De Lasa, p. 579. Nijhoff, The Netherlands.

Korsten, H. and Hoffmann, U. (1996) Three-phase reactor model for hydrotreating in pilot trickle-bed reactors. *A.I.Ch.E. J.* **42**, 1350.

Lee, H. H. and Smith, J. M. (1982) Trickle bed reactors: criteria for negligible transport effects and of partial wetting. *Chem. Engng Sci.* **37**, 223.

Leung, P. C., Recasens, F. and Smith, J. M. (1987) Hydration of isobutene in a trickle bed reactor: wetting efficiency and mass transfer, *A.I.Ch.E. J.* **33**, 996.

Levec, J. and Smith, J. M. (1976) Oxidation of acetic acid solutions in a trickle bed reactor. *A.I.Ch.E. J.* **22**, 159.

McNab, J. I. (1981) *Inst. Chem. Engng Symp. Ser.* **68**, 3/S:15.

Mata, A. R. and Smith, J. M. (1981) Oxidation of sulfur dioxide in a trickle bed reactor. *Chem. Engng J.* **22**, 229.

Mears, D. E. (1971) Tests for transport limitations in experimental catalytic reactors. *Ind. Engng Chem. Proc. Des. Develop.* **10**, 541.

Mills, P. L. and Dudukovic, M. P. (1980) Analysis of catalytic effectiveness in trickle bed reactors processing volatile or non-volatile reactants. *Chem. Engng Sci.* **35**, 2267.

Mills, P. L. and Dudukovic, M. P. (1981) Evaluation of liquid–solid contacting in trickle bed reactors by tracer methods. *A.I.Ch.E. J.* **27**, 893.

Mills, P. L. and Dudukovic, M. P. (1984) A comparison of current models for isothermal trickle bed reactors: application to a model reaction system. In *Chemical and Catalytic Reactor Modelling*, eds P. L. Mills and M. P. Dudukovic, p. 37. ACS.

Molga, E. J. and Westerterp, K. R. (1992) Kinetics of hydrogenation of 2,4 dinitrotoluene using a palladium on alumina catalyst. *Chem. Engng Sci.* **47**, 1733.

Montagna, A. A. and Shah, Y. T. (1975) The role of liquid holdup, effective catalyst wetting and backmixing on the performance of a trickle bed reactor for residue hydrodesulfurization. *Ind. Engng Chem. Proc. Des. Dev.* **14**, 479.

Mozingo, R. (1956) In *Organic Synthesis Collective*, Vol. 3, ed. E. C. Horning, p. 685. Wiley, London, U.K.

Neri, G., Musolino, M. G., Milone, C. and Galvagno, S. (1995) Kinetic modelling of 2,4 dinitrotoluene hydrogenation over Pd/C. *Ind. Engng Chem. Res.* **34**, 2226.

Nikalje, D. D. (1993) Ph.D. thesis, Shivaji University, Kohlapur, India.

Paraskos, J. A., Frayer, J. A. and Shah, Y. T. (1975) Effect of holdup, incomplete wetting and backmixing during hydroprocessing in trickle bed reactors. *Ind. Engng Chem. Proc. Des. Dev.* **14**, 315.

Ramachandran, P. A. and Chaudhari, R. V. (1983) *Three Phase Catalytic Reactors*. Gordon and Breach, New York, USA.

Ramachandran, P. A. and Smith, J. M. (1979) Effectiveness factors in trickle bed reactors. *A.I.Ch.E. J.* **25**, 538.

Sato, Y., Hiros, T., Takahashi, F. and Toda, M. (1973) Pressure loss and liquid holdup in packed bed reactor with cocurrent gas–liquid flow. *J. Chem. Engng Japan* **6**, 147.

Satterfield, C. N. (1975) Trickle bed reactors. *A.I.Ch.E. J.* **21**, 209.

Satterfield, C. N., Vab Eek, M. W. and Bliss, G. S. (1978) Liquid–solid mass transfer in packed beds with down flow cocurrent gas–liquid flow. *A.I.Ch.E. J.* **24**, 709.

Satterfield, C. N. and Way, P. F. (1972) The role of the liquid phase in the performance of a trickle bed reactor. *A.I.Ch.E. J.* **18**, 305.

Shah, Y. T. and Paraskos, J. A. (1975) Intraparticle diffusion effects in residue hydrodesulfurization. *Ind. Engng Chem. Proc. Des. Dev.* **14**, 368.

Shah, Y. T., Mhaskar, R. D. and Paraskos, J. A. (1976) Optimal quench location for a hydrodesulfurization reactor with time varying catalytic activity. *Ind. Engng Chem. Proc. Des. Dev.* **15**, 400.

Sicardi, S., Baldi, G., Gianetto, A. and Specchia, V. (1980) Catalyst area wetted by flowing liquid and semi stagnant liquid in trickle bed reactors. *Chem. Engng Sci.* **35**, 67.

Stephen, H. and Stephen, J. (1963) *Solubilities of Inorganic and Organic Compounds*, Part I, Vol. I, Table No. 1717, p. 543. Pergamon Press, U.K.

Tan, C. S. and Smith, J. M. (1980) Catalyst particle effectiveness with unsymmetrical boundary conditions. *Chem. Engng Sci.* **35**, 1601.

Valerius, G., Zhu, X., Hofmann, H., Arntz, D. and Haas, T. (1996) Modelling of a trickle bed reactor. II. The hydrogenation of 3-hydroxypropanal to 1,3 propanediol. *Chem. Engng Processing* **35**, 11.

Watson, P. C. and Harold, M. (1993) Dynamic effects of vaporization with exothermic reaction in a porous catalytic pellet. *A.I.Ch.E. J.* **39**, 989.

Watson, P. C. and Harold, M. (1994) Rate enhancement and multiplicity in a partially wetted and filled pellet: experimental study. *A.I.Ch.E. J.* **40**, 97.

Weast, R. C. and Astle, M. J. (1976) *CRC Hand book of Chemistry and Physics*. Chemical Rubber Co., Boca Raton, FL., U.S.A.

Westerterp, K. R., Janssen, H. J. and Van der Kwast, H. J. (1992) The catalytic hydrogenation of 2,4 dinitrotoluene in a continuously stirred three phase slurry reactor with an evaporating solvent. *Chem. Engng Sci.* **47**, 4179.

Wilke, C. R. and Chang, P. (1955) Correlation for diffusion coefficients in dilute solutions. *A.I.Ch.E. J.* **1**, 264.

Zai-Sha, M., Tian-Ying, X. and Chen, J. (1993) Theoretical predictions of static liquid hold up in trickle bed reactors and comparison with experimental results. *Chem. Engng Sci.* **48**, 2697.

Zheng Lu, P., Smith, J. M. and Herskowitz, M. (1984) Gas–particle mass transfer in trickle beds. *A.I.Ch.E. J.* **30**, 500.

APPENDIX

The dimensionless mass balance equations for species A in the three different zones are given as follows.

Dynamic zone:

$$-\frac{da_{l_d}}{dz}+\alpha_{gl_d}(1-a_{l_d})=\frac{L}{U_l}K_{ex}\varepsilon_{ls}(a_{l_d}-a_{l_s})+f_d\alpha_{ls_d}(a_{l_d}-a_{s_d}) \tag{A1}$$

and

$$f_d\alpha_{ls_d}(a_{l_d}-a_{s_d})=\frac{f_d\eta_c\alpha_r(b_l+k_{21}b_l+k_{31}c_l+k_{41}e_l)a_{s_d}}{(1+k_bb_l+k_cc_l+k_ee_l)} \tag{A2}$$

Stagnant zone:

$$\frac{L}{U_l} K_{ex}\varepsilon_{ls}(a_{l_d} - a_{l_s}) = f_s\alpha_{s_s}(a_{l_s} - a_{s_s}) = \frac{f_s\eta_c\alpha_r(b_l + k_{21}b_l + k_{31}c_l + k_{41}e_l)a_{s_s}}{(1 + k_bb_l + k_cc_l + k_ee_l)}. \quad \text{(A3)}$$

Dry zone:

$$(1 - f_d - f_s)\alpha_{s_g}(1 - a_{s_g}) = \frac{(1 - f_d - f_s)\eta_c\alpha_r(b_l + k_{21}b_l + k_{31}c_l + k_{41}e_l)a_{s_g}}{(1 + k_bb_l + k_cc_l + k_ee_l)}. \quad \text{(A4)}$$

Rearranging eq. (A4) we have

$$a_{s_g} = \frac{1}{\left[1 + \dfrac{\eta_c\alpha_r(b_l + k_{21}b_l + k_{31}c_l + k_{41}e_l)}{\alpha_{gs}(1 + k_bb_l + k_cc_l + k_ee_l)}\right]} \quad \text{(A5)}$$

the above equation reduces to

$$a_{s_g} = \frac{1}{(1 + \eta_c\phi^2/N_g)} \quad \text{(A6)}$$

where N_g and ϕ indicate the Nusslet number for gas phase and the dimensionless Thile parameter as shown in Table 5. In a similar way by considering eq. (A2) and repeating the same exercise we obtain

$$a_{s_d} = \frac{a_{l_d}}{(1 + \eta_c\phi^2/N_d)} \quad \text{(A7)}$$

where N_d represents the Nusslet number for liquid phase in the dynamic zone (see Table 5). From eq. (A3) we have

$$f_s\alpha_{s_s}(a_{l_s} - a_{s_s}) = \frac{f_s\eta_c\alpha_r(b_l + k_{21}b_l + k_{31}c_l + k_{41}e_l)a_{s_s}}{(1 + k_bb_l + k_cc_l + k_ee_l)}. \quad \text{(A8)}$$

Simplification of eq. (A8) leads to

$$a_{s_s} = \frac{a_{l_s}}{(1 + \eta_c\phi^2/N_s)}. \quad \text{(A9)}$$

In eq. (A9) N_s represents the Nusslet number for liquid phase in the static zone. Now eq. (A3) can be rewritten as

$$\frac{L}{U_l} K_{ex}\varepsilon_{ls}(a_{l_d} - a_{l_s}) = \frac{f_s\eta_c\alpha_r(b_l + k_{21}b_l + k_{31}c_l + k_{41}e_l)}{(1 + k_bb_l + k_cc_l + k_ee_l)} \times \frac{a_{l_s}}{(1 + \eta_c\phi^2/N_s)}. \quad \text{(A10)}$$

Simplification of eq. (A10) leads to

$$a_{l_s} = \frac{a_{l_d}}{\left[1 + \dfrac{f_s\eta_cWk_1B_l(b_l + k_{21}b_l + k_{31}c_l + k_{41}e_l)}{K_{ex}\varepsilon_{ls}(1 + \eta_c\phi^2/N_s)(1 + k_bb_l + k_cc_l + k_ee_l)}\right]}. \quad \text{(A11)}$$

Equation (A11) can also be expressed as

$$\frac{a_{l_s}}{(1 + \eta_c\phi^2/N_s)} = \frac{a_{l_d}}{[1 + \eta_c\phi^2/N_s + (\eta_c\phi^2/\alpha_sN_s)]} \quad \text{(A12)}$$

Now eq. (A10) is reproduced as

$$\frac{L}{U_l} K_{ex}\varepsilon_{ls}(a_{l_d} - a_{l_s}) = \frac{f_s\eta_c\alpha_r(b_l + k_{21}b_l + k_{31}c_l + k_{41}e_l)}{(1 + k_bb_l + k_cc_l + k_ee_l)} \times \frac{a_{l_d}}{[1 + \eta_c\phi^2/N_s + (\eta_c\phi^2/\alpha_sN_s)]} \quad \text{(A13)}$$

Hence, the overall dimensionless mass balance equations for species A by taking into consideration the above modifications can be given as

$$-\frac{da_{l_d}}{dz} + \alpha_{gl}(1 - a_{l_d}) = \frac{\eta_c\alpha_r(b_l + k_{21}b_l + k_{31}c_l + k_{41}e_l)}{(1 + k_bb_l + k_cc_l + k_ee_l)} \times \left\{\frac{f_da_{l_d}}{(1 + \eta_c\phi^2/N_d)} + \frac{f_sa_{l_d}}{\left[1 + \dfrac{\eta_c\phi^2}{N_s} + (\eta_c\phi^2/\alpha_sN_s\right]}\right\} \quad \text{(A14)}$$

$$(1 - f_d - f_s)\alpha_{gs}(1 - a_{s_g}) = (1 - f_d - f_s) \times \frac{\eta_c\alpha_r(b_l + k_{21}b_l + k_{31}c_l + k_{41}e_l)}{(1 + k_bb_l + k_cc_l + k_ee_l)}\left[\frac{1}{(1 + \eta_c\phi^2/N_g)}\right]. \quad \text{(A15)}$$